Proceedings of the ASME 2010 3rd Joint US-European Fluids Engineering Summer Meeting and
8th International Conference on Nanochannels, Microchannels, and Minichannels
FEDSM-ICNMM2010
August 1-5, 2010, Montreal, Canada

FEDSM-ICNMM2010-3$(')

A DETAILED OBSERVATION OF HYDROFOIL CAVITATION AND A PROPOSAL FOR IMPROVING CAVITATION MODEL

Motohiko Nohmi
EBARA Corporation
Futtsu-shi, Chiba, Japan

Naoya Ochiai
Graduate School of Engineering,
Tohoku University
Sendai, Miyagi, Japan

Yuka Iga
Institute of Fluid Science, Tohoku University
Sendai, Miyagi, Japan

Toshiaki Ikohagi
Institute of Fluid Science, Tohoku University
Sendai, Miyagi, Japan

ABSTRACT

Cavitation of a hydrofoil is observed in detail by using a high speed video camera. A paint removal test is also carried out in order to evaluate cavitation aggressiveness for erosion. 2D hydrofoil profile is Clark Y 11.7% and its angle of attack is seven degrees. Cavitation number is $\sigma=1.08$. The experimental results are compared with cavitation CFD. Numerous features of unsteady cavitation are observed such as cyclic fluctuation of the sheet cavity, existence of the glassy cones on a sheet cavity, generation of the cloud cavitation from the sheet cavity and the isolated bubbles traveling over the suction surface of the blade. The isolated traveling bubbles and their collapses are thought to be one of the main causes of the severe paint removals. The isolated traveling bubbles are derived from the flowing cavitation nucleus or from abrupt onset at the leading edge of the blade. For computing these complicated phenomena, combination of grid scale bubbles (GSB) and sub grid scale bubble model (SGSB) are proposed. GSB shall be computed by using the computational scheme for the free surface with phase change model. SGSB can be computed with conventional cavitation model. The breakup of GSB generates SGSB, and the coalescence of SGSB makes GSB. Upper limit of void fraction of SGSB is estimated in the range of five or ten percent from the simple speculation of the structure of packed spheres. The two types of cavitation bubble inception model are also discussed based on the generation of the isolated bubbles observed in the experiments. To verify the proposed concepts of cavitation model, a traveling air bubble over a hydrofoil is computed by using the free surface flow scheme of Volume of Fluid (VOF) approach. Cavitation on the hydrofoil
is also computed by VOF approach with boiling model concerning the heat transfer. Both the computed results show qualitatively similar characteristics of the bubble dynamics to those in experimental results.

INTRODUCTION

Recently some numerical approaches for the prediction of cavitation erosion were proposed (Dular et al.(2006), Franc (2009), Fukaya et al.(2009), Fortes-Patella(2001), Berchiche et al.(2001)). The authors proposed the two kinds of methods applied for the cavitation on 2D hydrofoil profile of Clark Y 11.7% in the previous papers (Nohmi(2008), Ochiai(2009)). For the validation of the proposed methods, cavitation of the hydrofoil is observed in detail by experiments. There have been many important investigations about the comparison of the experimental results and CFD results for cavitating hydrofoil (for examples of the latest in CAV2009 Wang et al.(2009), Zima et al.(2009), Seo et al.(2009), Peng et al(2009)) In this research, due to the accidental nonuniformity of the incoming flow, numerous features of the unsteady three dimensional cavitation such as partially wetted blade, traveling bubbles and cloud cavity shedding are observed. There is a discrepancy between the observed paint removal and the predicted erosion aggressiveness, however the important roll of the traveling bubbles for erosion are clarified. Based on the experimental observation, debatable points of the present modeling of cavitation for CFD are discussed. For computing these complicated unsteady cavitation phenomena more accurately, the combination of grid scale bubbles and sub grid scale bubble

model are proposed and the preliminary computations were carried out.

NOMENCLATURE
    p   pressure
    p_v saturation vapor pressure
    T_c time cycle of break off of sheet cavity
    VOF   volume ratio of gas phase for the VOF scheme
    α void fraction
    σ cavitation number

EXPERIMENTAL APPARATUS

    A closed type cavitation tunnel was constructed. It consists of a reservoir tank, a centrifugal pump, test section that contains the hydrofoil and a controlled valve. The tank is connected to vacuum pump in order to control cavitation number. Volume flow rate is measured using a magnetic flow meter. A schematic of the facility is shown in Fig.1. The test section is a rectangular channel and its cross section is 120mm by 70mm and the chord length of the hydrofoil is 70mm. Angle of attack is fixed to seven degrees. In accordance with the flow condition of the previous CFD, area averaged velocity at the cross section is 10m/s for most of the test experiments. For the calculation of the area averaged flow velocity, the volume flow rate is simply divided by the area of the rectangular channel. Cavitation number that is measured just downstream of the hydrofoil is about σ=1.08. The low velocity experiments of area averaged velocity 8m/s is also carried out for easier observation. Tip clearance between hydrofoil and the wall of the test section is caulked by using silicon rubber membrane that has the same profile with the hydrofoil and the tip leakage flow is prevented. The water inside the cavitation tunnel is deaerated. Its dissolved oxygen is in the range of 6 to 7 mg/l. The water temperature is kept in the range of 12 to 18 degrees centigrade.
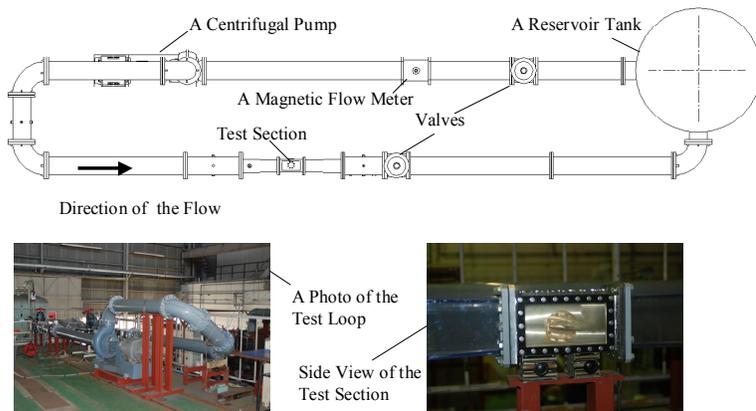
Fig.1 A Top View of the Schematic of the Experimental Apparatus

The suction surface of the hydrofoil is painted blue by using layout dye for the evaluation of the cavitation erosion aggressiveness. Unsteady cavitation characteristics are observed in detail by using a high speed video.

NUMERICAL ANALYSES

    In this study, the unsteady 2D cavitation flow is computed by using the code developed by Institute of Fluid Science, Tohoku University. Detailed information of this code is available in the previous paper (Nohmi et al., 2008). A commercial code with cavitation model, ANSYS-CFX is also used. A computation of a single air bubble flowing around the hydrofoil is carried out as a preliminary study of the cavitation model improvement by using ANSYS-FLUENT with VOF method. Another preliminary study is the computation of hydrofoil cavitation by using VOF method with boiling model concerning heat transfer at room temperature. In this calculation, a commercial code Star-CD is used.

RESULTS AND DISCUSSIONS

    Experimental Results Fig.2 shows a snap shot of a sheet cavity. Based on the side view using the high speed video, a portion of the upstream part of the sheet cavity appeared to be glassy. The downstream part of the sheet cavity (not glassy) extended downstream to the trailing edge of the hydrofoil. There is a vortex structure at the aft portion of the sheet cavity (Fig.2). As the aft edge of the sheet cavity approaches the trailing edge of the hydrofoil, the vortex grows rapidly. When the aft edge of the sheet cavity reaches the trailing edge of the hydrofoil, the vortex is shed downstream as a cloud cavity. Then the fore part of the sheet cavity that remains on the blade shrinks upstream rapidly. The shedding of the cloud cavity does not always necessitate the reach of the aft edge of the sheet cavity to the trailing edge of the hydrofoil. After the two or three times of the cloud cavity shedding, the sheet cavity shrinks upstream rapidly and disappears. For a very short moment, the suction surface of the blade is almost fully wetted(Fig.3).
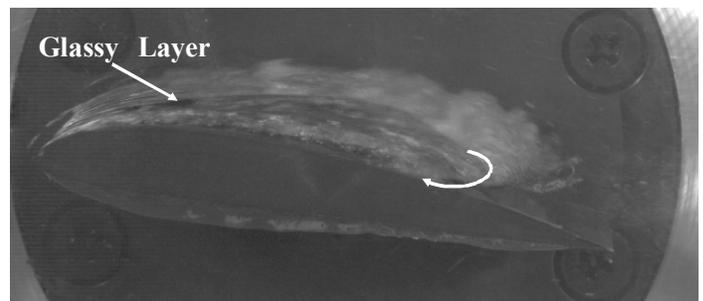
Fig.2 The Glassy Layer and the Vortex at Trailing Edge of Sheet Cavity, a side view of the Hydrofoil and the flow is from left to right
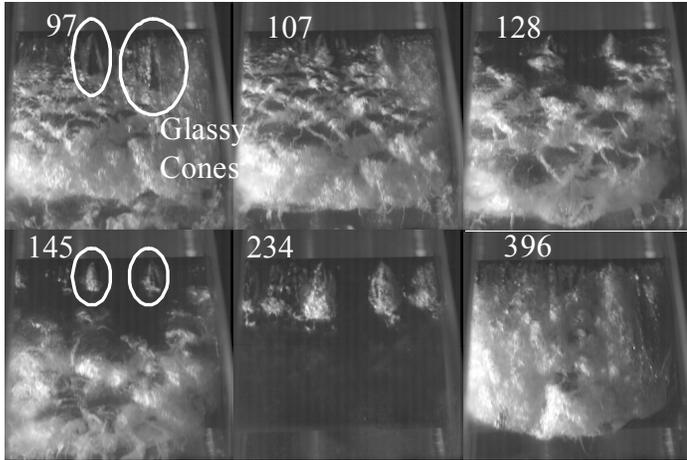
Fig.3 Cyclic Disappearance of the Sheet Cavity and the Glassy Cones, a top view of the Hydrofoil and the flow is from top to bottom

After the fully wetted moment, the sheet cavity is reborn. The existence of fully wetted moment for the hydrofoil cavitation is also reported by Williams et al.(2009). They suggested this phenomenon can be strongly affected by the surface characteristics of the blade. In this study, the blue paint over the blade might have some effects. Even when the blade surface is fully wetted, the remains of the bubbles from cloud cavity still exist around the blade. The principal components of these remained bubbles might not be vapor but oxygen and nitrogen released from the water. At the fore part of the sheet cavity, there are relatively large glassy transparent cones those look filled with single phase gas. These glassy cones are similar to the structure reported by Leger et al.(1998) and Bouziad et al.(2003). In many cases, the glassy cones look starting from the leading edge of the blade. These cones stand relatively stable while the sheet cavity exists. The glassy part in the sheet cavity seen in Fig.2 is thought to be the side view of a glassy cone. Reverse flow in also observed inside the glassy cone. When the reverse flow reaches the leading tip of the glassy cone, the glassy cone is broken up to the small clouds of bubbles. Just after the break up of the glassy cone, a new glassy cone is often reborn at the almost same position (Fig.3). This may be a kind of rebound. Moreover the glassy cones may correspond to some sort of surface imperfection or scratch, however in these experiments there were not clear evidences The leading edge of the sheet cavity is not straight but wavy (Fig.4). On the wavy structure, a finger like bifurcation occurs cyclically and fingers are propagated in span wise direction over the wave peaks. Similar cyclic bifurcation is also observed around the glassy cones. The sheet cavity shows cyclic fluctuation as written above. From the FFT analyses of the pixel brightness in particular location in the movie frames, primary frequency of the fluctuation is 20-21 Hz and there are second and third harmonic peaks in the spectrum.
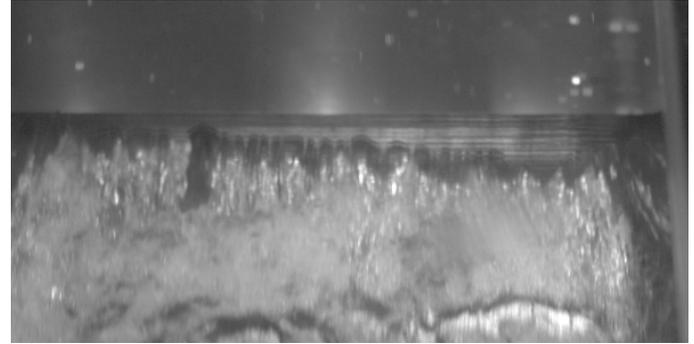
Fig.4 The Wavy Leading Edge of the Sheet Cavity, a top view of the Hydrofoil and the flow is from top to bottom

The primary frequency corresponds to the cycle time of the appearance of the fully wetted moment and the harmonics derive from the cloud cavity shedding. The high speed video movie of the top view also shows that the sheet cavity appears earlier at the left side of the blade and grows to the right side of the blade as seen in Fig.5. This may be due to the nonuniformity of the incoming flow velocity. There are three elbows upstream of the test section as seen in Fig.1 and there are not any stratification devices. CFD computation for the upstream flow concerning the elbows shows higher velocity at the left side of the blade. This means the local cavitation number at the left side of the blade is lower and the cavitation tends to appear much easier.
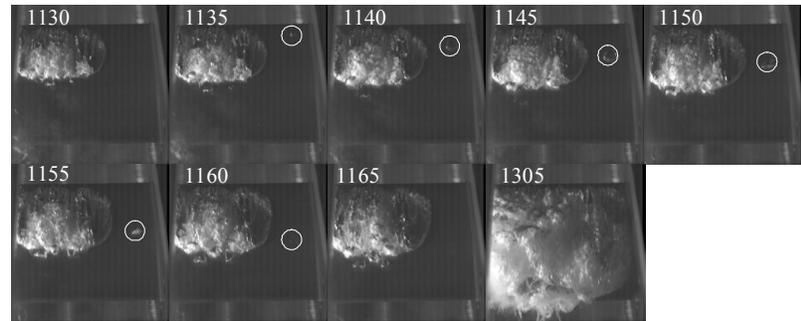
Fig.5 The Traveling Bubble and its Collapse on the partially Wetted Area, a top view of the Hydrofoil and the flow is from top to bottom

Fig.6 shows an example of the photos of removed paint on the blade. Paint is removed severely at the midchord of the blade, particularly right side and right corner (as seen I in Fig.6). Paint removal is also observed at the aft part of the blade tip (II in Fig.6). Paint at the midspan near the trailing edge of the blade is also removed slightly (III in Fig.6). High speed video of the top view clarifies the mechanism of the paint removal. After the fully wetted moment, the left side of the blade is soon covered by sheet cavity.
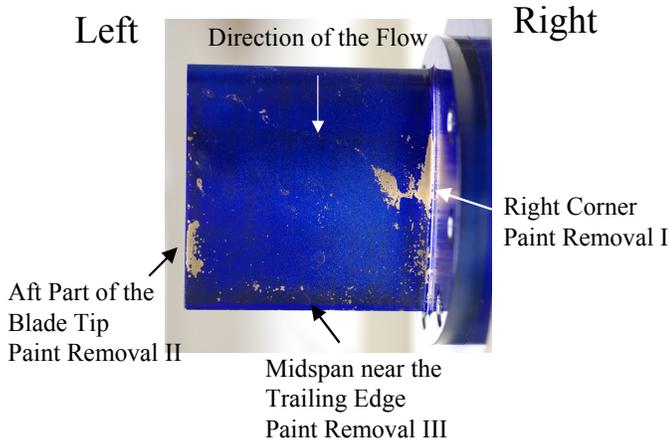
Fig.6 Removed Paint due to Cavitation, a top view of the Hydrofoil

Fig.7 A Nucleus Approaching the Leading Edge of the Blade and Its Transformation to Traveling Bubble on the Blade, a top view of the Hydrofoil and the flow is from top to bottom

Fig.8 Abrupt Onset of a Traveling Bubble and its Finger-like Bifurcation, a top view of the Hydrofoil and the flow is from top to bottom

However the right side of the blade is wetted for a while until the sheet cavity extends to the right corner of the blade (see Fig.5). In this partially wetted moment, the traveling bubbles sometimes flow over the right side of the blade and collapse around the paint removed area. These traveling bubbles are isolated or dispersed. A traveling bubble is seen in the circle of Fig.5. After the collapse, the rebound of the bubble is also observed in some high speed movies. At the leading edge of the right side of the blade, cavitation often appears. This leading edge cavitation also causes the traveling bubbles downstream and these traveling bubbles collapse at the midchord corner of the blade. These collapse of the traveling bubbles are thought to be the cause of severe paint removal at the right side of the blade (I in Fig.6). The aft part of the blade is cyclically covered with the trailing part of the sheet cavity and the shed cloud cavities. Many of the bubbles in the cloud cavities collapse around the trailing edge of the blade and probably cause the paint removal (III in Fig.6). Paint removal at the aft part of the blade tip (II in Fig.6) are probably caused by relatively long time contact with the vortex cores of the sheet cavities and the cloud cavities.

Further observations were carried out to analyze the origin of the traveling bubbles over the blade surface. Area averaged flow velocity is decreased to 8m/s and the leading edge of the blade is observed in detail. There are at least two mechanism of the generation of the traveling bubbles. Fig.7 shows the cavitation nucleus that approaches the leading edge of the blade begins to travel over the blade surface. In this study the detailed measurement of the nucleus size was not carried out. From the figures in the high speed video movies, its typical size is roughly estimated in the range of sub mm. Another mechanism is an abrupt onset of a traveling bubble around the leading edge of the blade as seen in Fig.8. In the approaching nucleus cases, sometimes nucleus decrease their velocity just upstream the leading edge of the blade.
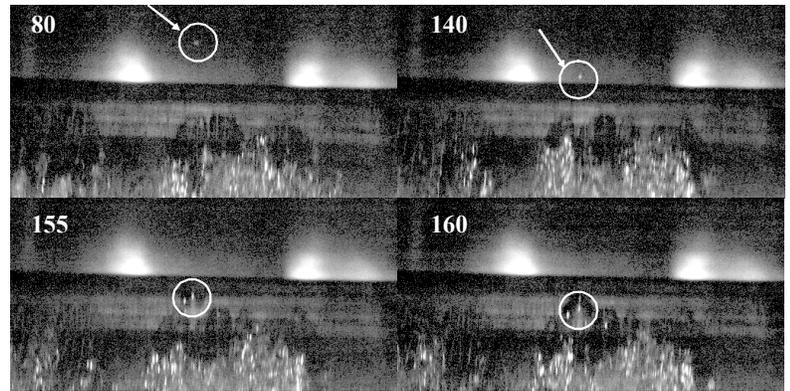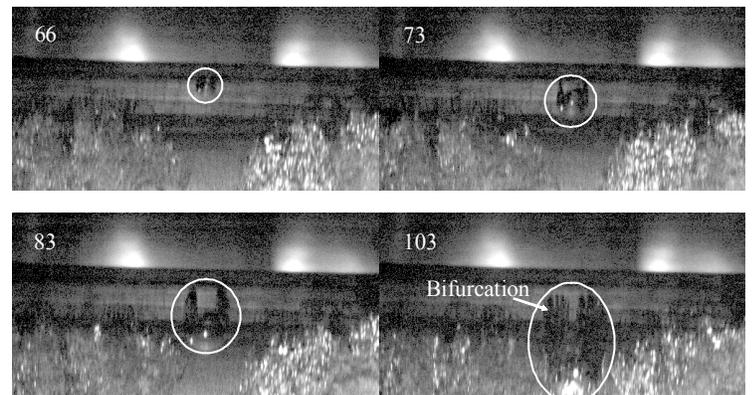
It may be the reason of this deceleration that nuclei are on the stagnation streamline toward the leading edge of the blade or on the trajectories very close to the stagnation streamline. If the nuclei are on the stagnation streamline, they decrease the velocity around the stagnation point. If the nucleus trajectories are very close to the stagnation streamline, the trajectories are quite turned around the leading edge of the blade, and the mainstream component of the nucleus velocity decreases very much. The abruptly generated bubbles on the blade may be derived from nucleate boiling on site or from the incoming nuclei those are too small to be photographed by the high speed video with limited resolution. Abruptly generated bubbles are however not necessarily smaller than the bubbles those are clearly derived from the incoming visible nuclei. So random nucleate boiling like phenomena are highly probable for making the bubbles on the blade abruptly. In Fig.8, a traveling bubble shows fingerlike bifurcation. This bifurcation is noted as "streaks or tails" by Brennen (Brennen,2005). He suggested that "when a bubble passed a point of laminar separation, it

triggered the formation of local attached cavitation streaks at the lateral or spanwise extreamities of the bubble." In this study, the flow is not in the incipient cavitation condition and is highly perturbed by the existent sheet cavities. It is not clear that the stable laminar separation does exist. Further research is necessary.
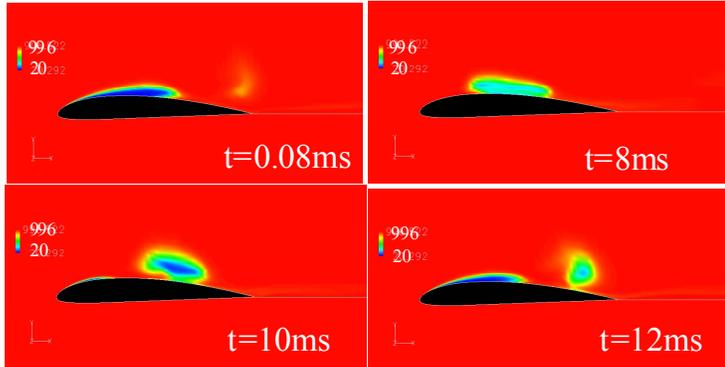
Fig.9 Cavitating Flow Field with Periodic Fluctuation
(Density Contour, unit:kg/m^3)
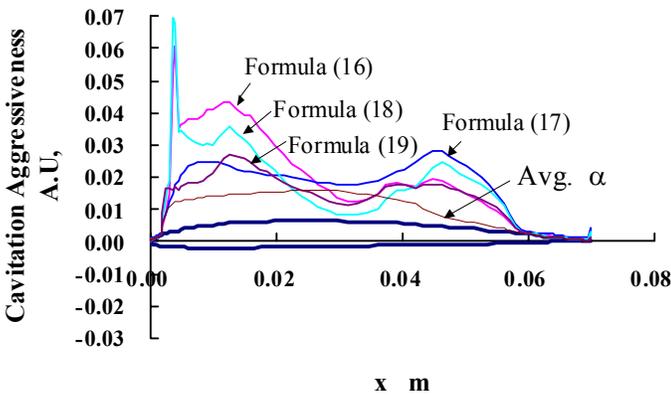
$$\frac{1}{T_c}\int_0^{T_c}\alpha\cdot\max[\frac{\partial p}{\partial t},0]dt \qquad (16) \qquad \frac{1}{T_c}\int_0^{T_c}\alpha\cdot\max[(p-p_v),0]dt \qquad (17)$$

$$\frac{1}{T_c}\int_0^{T_c}p\cdot\max[-\frac{\partial\alpha}{\partial t},0]dt \qquad (18) \qquad \frac{1}{T_c}\int_0^{T_c}\max[-\frac{\partial\alpha}{\partial t},0]dt \qquad (19)$$

Fig.10 Calculated Cavitation Aggressiveness

Comparison between Experiments and CFD Fig.9 and Fig.10 show the result of unsteady cavitation CFD and estimated cavitation erosion aggressiveness from the previous paper (Nohmi et al.,2008). The four types of cavitation erosion aggressiveness were proposed as described in the equations in Fig.10. The equation numbers are same in the previous paper. These are simple combination of the higher void fraction, the

higher pressure in the cavitation region, the higher collapsing rate of void fraction and the higher rate of pressure rise in the cavitation region. These values on the blade surface are temporally integrated in the time range of cloud cavity shedding. In the unsteady CFD, the whole sheet cavity is separated from the blade when the re-entrant jet from the trailing part of the sheet cavity reaches the leading part of the sheet cavity. Then sheet cavity is separated from the blade surface and is shed downstream as a cloud cavity. Water hammer pressure rise is generated at the leading part of the sheet cavity just before its separation from the blade. Due to this high pressure water hammer pulse, the cavitation aggressiveness is very high in the estimations of Eq.(16) and Eq.(18) in Fig.10. However the cavitation aggressiveness in the experiment is highly three dimensional and differs from the estimation as seen in Fig.6. The three dimensionality discussed in the previous section cannot be predicted by 2D CFD of course. Another discrepancy between experiment and CFD is the cloud cavitation. In the experiments, only the aft part of the sheet cavities are shed and the separation of the whole sheet cavity from the blade is not observed. For comparison, the same flow is also computed unsteadily by ANSYS-CFX using a SST turbulence model and the same numerical grids. The snapshot of this result is seen in Fig.11.
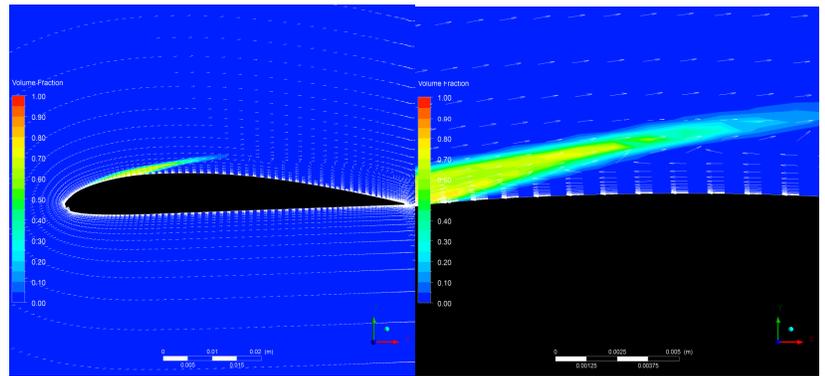
Fig. 11 2D unsteady computation by ANSYS-CFX with SST turbulence model, Contour of void faction and velocity vectors, Right figure is a close up of the left figure
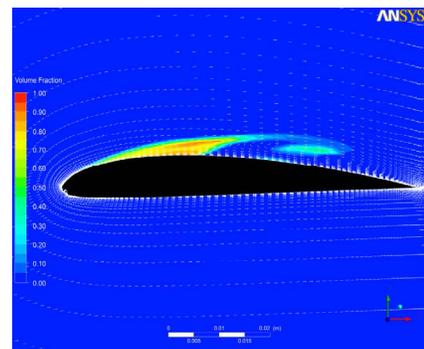
Fig. 12 2D LES computation by ANSYS-CFX, Contour of void faction and velocity vectors

In this case, the sheet cavity fluctuates cyclically, however the cloud cavity is not shed. It is noticeable that a large separation vortex exists downstream the sheet cavity in Fig.11. This type of vortex is discussed in detail in the paper (Hoekstra at al. 2009). Many researchers suggest that too much eddy viscosity in two phase region in RANS-cavitation CFD ceases the unsteady dynamic behaviors of cavitation such as cloud cavity shedding. Empirical reduction of the eddy viscosity is often adopted. In this study, although the appropriateness of 2D LES is controversial, 2D computation of both laminar approximation and LES are carried out. Fig.12 shows LES results. In Fig.12 the large separation vortex downstream the sheet cavity is also cavitated and is shed cyclically. The computational result in Fig.12 looks as if the aft part of the sheet cavity is shed as seen in the experiments. The laminar computation shows the cloud cavity shedding, however is more unstable compared to the LES computation (Nohmi et al.,2009). 3D computation by ANSYS-CFX is also carried out and shows the cloud cavity shedding even in the case of RANS computation (Nohmi et al.,2009). Further computation, experimental observation and the discussion should be continued in order to clarify the three dimensional mechanism of the cloud cavity shedding.

A Proposal for improving Cavitation Model Various cavitation models have been proposed. For examples, methods concerning free surfaces between gas phase and liquid phase, one fluid model (one density and one velocity ignoring interphase slip), two fluids model, methods assuming continuum phase of liquid and dispersed phase of gas bubbles smaller than grid size concerning their interaction and so on. It should be noted that the terminology about cavitation model is not fixed (for example, see Goncalves et al. (2009)). One fluid model is widely adopted by the researchers in academia and by commercial CFD code vendors. In many of one fluids model, the phase change is considered by adding the source term to the conservation equation of density, void fraction, or steam quality and so on. Source term is typically the function of $(p-p_v)$ or $(p-p_v)^{0.5}$ (Frikha et al.,2008). If the pressure that is defined in the locally homogeneous medium decreases less than saturated vapor pressure computed based on local temperature, then evaporation starts and vice versa. By using this kind of cavitation model and steady computational scheme, many interesting characteristics such as pump head breakdown can be somewhat calculated. However for computing complicated unsteady cavitation phenomena as described in the previous section, modification of the cavitation model is mandatory. For example, local void fraction is defined in one fluid model. However in the real situation, void fraction is defined as spatially averaged gas phase volume in unit volume and is highly dependant on the size and the location of control volume. This fact has conflict with another fact (expectancy?) that accuracy of numerical computation is ordinarily improved by decreasing the size of grids. Strictly speaking one fluid model falls apart if the grid size becomes smaller than the

bubble size. Large bubbles those cannot be ignored compared to the chord length of the blade are often observed in experiments such as glassy cones in Fig.3. For solving this problem, grid scale bubbles (GSB) should be calculated by using interface tracking or capturing methods such as VOF method, Level Set method, immersed boundary method and so on concerning the phase change and surface tension at the interface. Simultaneously sub grid scale bubbles (SGSB) should be computed by the scheme of ordinary one fluid or two fluids model. Whole cavitation flow field is computed by the combination of GSB and SGSB. This hybrid approach has been already proposed (Kawamura et al.(2003), Masuda et al.,(2007),Apte et al.,(2009)).
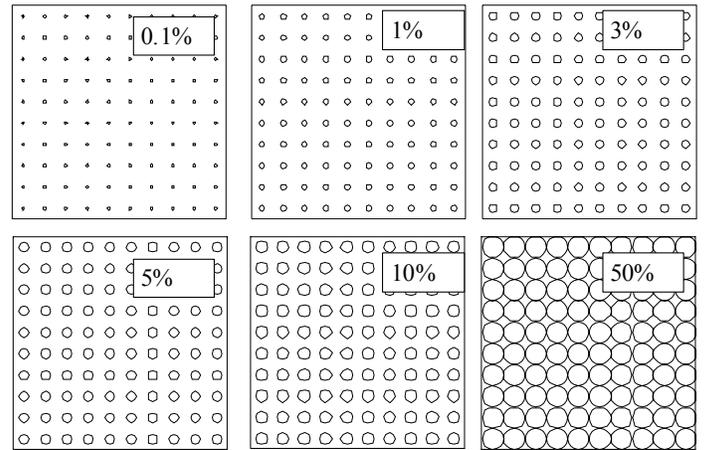
Fig.13 Void Fraction of Simple Cubic Lattice of Bubbles

Void fraction of SGSB shall be discussed quantitatively. It is well known that water becomes clouded by adding air bubbles of one percent void fraction. Fig. 13 shows spatial occupation of spherical bubbles in the assumption of simple cubic lattice. From Fig.13 void fraction of 50% or greater cannot be realistic. (It could be possible with some surfactant.) Comparing the high speed video of cavitation and Fig.13, the maximum of the instantaneous void faction of the bubbly region is estimated less than five or ten percent. Sometimes high void fraction of 50,70 or 90 % is evaluated as contour surface for CFD results, however such high value is not realistic for almost homogeneous bubbly region. Of course void fraction inside the large bubbles can be said 100 %. (So, local void fraction greater than 10% is reasonable for the temporally averaged flow and can be evaluated by steady computation or by temporally averaged unsteady computation. See Fig.14) From this discussion, modeling shall be as follows.
  (1) Instantaneous void fraction is discontinuous.
  (2) Instantaneous void fraction for GSB region is 100%.
  (3) Instantaneous void fraction for SGSB region is less than some threshold say 10%.
  (4) When void fraction of numerical cells or grids for SGSB region becomes larger than the threshold, GSB

is born and grows up. This simulates for examples generation of the sheet cavities, generation of the visible core of cavitation vortices and so on.

(5) SGSB is formed from the surface breakup of GSB based on some criteria such as, surface shear stress, surface tension, surface radius, pressure gradient around the surface, Kelvin-Helmholtz instability, Rayleigh-Taylor instability and so on.

(6) SGSB is adsorbed to GSB, when SGSB collide with GSB

The concepts above mentioned are drawn as seen in Fig. 15. The detailed modeling of SGSB formation from GSB surfaces could be inspired by some atomization modeling (Reitz,1987).
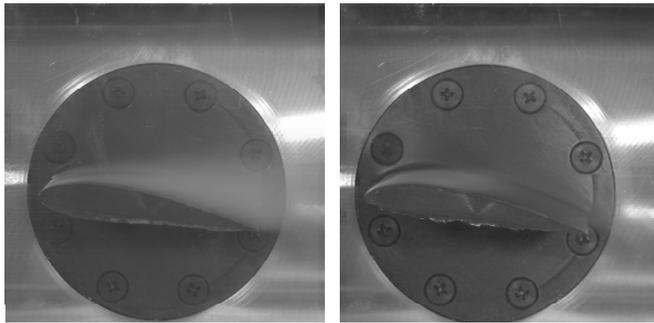
(a) Velocity 10m/s   (b) Velocity 8m/s

Fig.14 Temporally averaged figures of the high speed movie frames
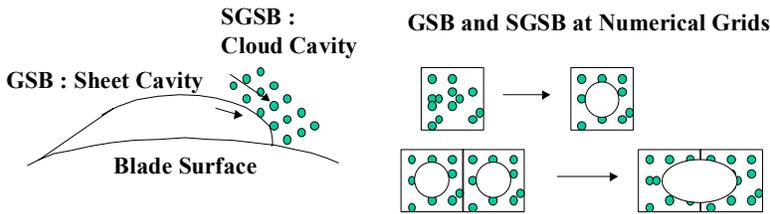
(a) Breakup of GSB forming SGSB   (b) Coalescence of SGSB forming GSB

Fig.15 A Schematic Model of the Interaction of GSB and SGSB

Modeling of the incipient process of cavitation would be discussed. In many of the source term type cavitation modeling, sign of (p-p$_v$) would be the criterion of cavitation generation. However by ordinary, saturation vapor pressure is the value under the equilibrium condition of evaporation and condensation with flat interface between water phase and vapor phase. Fundamentally it cannot be applied for the unsteady process and also for the curved interface. Moreover water withstands tensile stress instantaneously. Bouziad et al. measured the tensile stress in the hydrofoil cavitatin experiments (Bouzuad et al.,2003). So the deterministic algorithm based on (p-p$_v$) shall be modified. The incipient process can be modeled based on the experimental observation

in Fig.7 and Fig.8. Randomly incoming nuclei are modeled by using randomized GSB or cluster of SGSB cells or grids. The model of randomized nucleate boiling is also applicable for incipient process (Saito et al.,2000). Concerning the conservation of energy, thermodynamic effects of cavitation is reasonably counted in these modelings. It is argued that mist could be formed inside a vapor bubble because of the temperature decrease due to latent heat (Takemura et al.,1992). Model of sub grid scale mist inside GSB may be necessary. With some surface tension, GSB and SGSB withstand negative pressure medium. If liquid water is assumed incompressible, it is no problem to calculate the tensile stress. On the other hand, under the assumption of compressible liquid water, the state equation of water such as Tait's may be extrapolated to negative absolute pressure range.

Preliminary computations of improved Cavitation Model In this study two kinds of preliminary computation are carried out particularly for the evaluation of GSB approach. First, single air bubble approaching the hydrofoil is analyzed by GSB model. ANSYS-Fluent is applied with interface capturing by VOF method. The mainstream velocity and the angle of attack are matched to the experiments. However cavitation is not considered and any cavitation model is not applied for computation. Water is assumed incompressible and air inside the bubble is assumed compressible and isothermal. RNG K-ε model is adopted for turbulence closure. Surface tension is considered. Initial diameter of bubble is 1mm. At first, the steady flow without bubble is computed for setting initial condition. Then the spherical bubble with same pressure and same velocity with the result of initially calculated water flow is released in surrounding water flow. Fig.16 shows the result of 2D computation. The bubble decreases the velocity around the stagnation point then starts to flow over the suction surface. The bubble expands at the low pressure region and continues cyclic shrinking and rebounds with breaking up and coalescence. These characteristics are quite similar to the behavior of cavitation bubble in Fig.5 and Fig.7. The result of 3D computation is seen in Fig.17. In this figure traveling bubble over the blade surface breaks up in spanwise direction. This spanwise breaking up may correspond to the fingerlike bifurcation in Fig.8 qualitatively.

Another preliminary computation is the cavitation on the blade by using interface capturing with VOF method. Star-CD is applied because of its VOF scheme with phase change. In this computation, in stead of cavitation model, boiling model is adopted for the phase change at room temperature. Conservation of energy and heat transfer are considered. For boiling model, not the saturation vapor pressure but the temperature of boiling point is used as the threshold of phase change in the scheme. The temperature of boiling point is calculated under the assumption of local equilibrium. However this assumption might not be appropriate as discussed above. Compressible computation is quite unstable so both water and vapor are assumed incompressible.

7   Copyright © 2010 by ASME
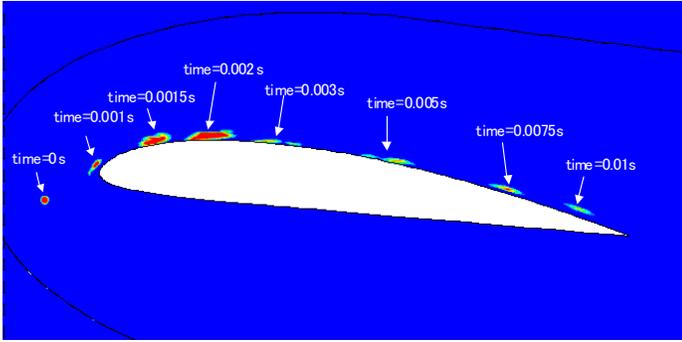
Fig.16 Computed Result of a Traveling Bubble over the Suction Surface (2D case), a Contour of the void fraction
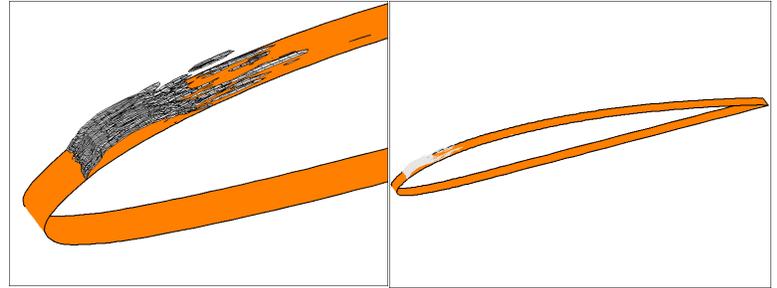
Fig.17 Computed Result of a Traveling Bubble over the Suction Surface (3D case)

The mainstream velocity and the angle of attack are matched to the experiments. Pressure level and overall temperature in the flow field is so selected that minimum pressure at the suction surface is slightly less than saturation vapor pressure. Overall temperature is 20 degrees centigrade. Surface tension is considered as artificial body force effective at the cells of VOF=0.5. Due to the limitation of the computer resources, spanwise length is just 20mm. Boundary condition of the "side wall" is slip wall. RNG K-ε model is adopted. The snapshot of the unsteady computation is seen in Fig.18. The characteristic of computed "boiling" is fixed bubble with the shedding of traveling bubbles. The leading part of the bubble of VOF=0.5 shows wavy curve that is similar to the results in experiments as seen in Fig.4. Surface tension might be the cause of this wavy curve in computation. Perhaps in experiments, the effect of turbulence is also important for this wavy structure. The region of VOF=0.1 is much larger than that of VOF=0.5. It looks somewhat like supercavitation. So big region of lower value of VOF may be due to the too much numerical diffusion in the conservation of VOF. Sharp gradient of VOF value would be ideal for high resolution of the captured interface.

From the results of both preliminary computations, it could be said that considering the surface tension is important for computing the complicated phenomena of cavitation.

(a) Isosurface of VOF=0.5

(b) Isosurface of VOF=0.1

Fig.18 Computed Result of "Boiling" over the Suction Surface

Although further study and validation are necessary, the results of both preliminary computations might show that the proposed improvement of cavitation model is on the right track.

CONCLUSIONS

Cavitation of a hydrofoil is analyzed in detail by using a high speed video camera and paint removal test. Numerous features of unsteady cavitation are observed such as cyclic fluctuation of the sheet cavity, existence of the glassy cones on a sheet cavity, generation of the cloud cavitation from the sheet cavity and the isolated bubbles traveling over the suction surface of the blade. Experimental results are compared with cavitation CFD. For improving cavitation model, the concepts of the combination of grid scale bubble and sub grid scale bubble are discussed. The preliminary computations for the evaluation of the proposed concepts show the similarity to the experimental results

REFERENCES

(1) Dular M. et al., 2006, "Experimental and Numerical Modeling of Cavitation Erosion",CAV2006, Wageningen

(2) Fortes-Patella et al., 2001, "Cavitation Erosion Mechanism : Simulations of the Interaction between Pressure Waves and Solid Boundaries", CAV2001, California

(3) Fukaya M. et al., 2009, "Prediction of Impeller Speed Dependence of Cavitation Intensity in Centrifugal Pump Using Cavitating Flow Simulation with Bubble Flow Model", CAV2009 Ann Arbor, Paper No.15

(4) Franc J.P. et al, 2009, "Incubation Time and Cavitation Erosion Rate of Work-Hardening Materials", JFE.Vol.131 February,021303

(5) Berchiche N. et al., 2001, "A Cavitation Erosion Model for Ductile Materials", CAV2001, California

(6) Nohmi M. et al., 2008," Numerical Prediction Method of Cavitation Erosion",FEDSM2008-55126

(7) Ochiai N. et al.,2009," Numerical Prediction of Cavitation Erosion in Cavitating Flow", CAV2009 Ann Arbor, Paper No.67

(8) Wang G. et al.,2009,"Unsteady Dynamics of Cloud Cavitating Flows around a Hydrofoil", CAV2009 Ann Arbor, Paper No.9

(9) Zima P. er al.,2009, "Modeling collapse aggressiveness of cavitation bubbles in hydromachinery", CAV2009 Ann Arbor, Paper No.131

(10) Seo J. H. et al.,2009, "Numerical investigation of cloud cavitation noise on a hydrofoil section", CAV2009 Ann Arbor, Paper No.62

(11) Peng X. et al.,2009, "Observations and numerical simulations of unsteady partial cavitation on 2-d hydrofoil", CAV2009 Ann Arbor, Paper No.164

(12) Williams M. et al., 2009, "Effects of Surface Characteristics on Hydrofoil Cavitation", CAV2009 Ann Arbor, Paper No.112

(13) Leger et al.,1998,"Examination of the flow near the leading edge of attached cavitation. Part2. Incipient breakdown of two-dimentional and axisymmetric cavities" „J. Fluid Mech., Vol.376,pp.91-113

(14) Bouziad Y.V. et. al.,2003,"Numerical Simulation of Leading Edge Cavitation",FEDSM2003-45312

(15) Brennen, C.E.,2005, ``Fundamentals of Multiphase Flow''. Cambridge University Press,pp139-142

(16) Hoekstra M.,"The partial cavity on a 2D foil revisited", CAV2009 Ann Arbor, Paper No.43

(17) Nohmi M. et al.,2009,"A Detailed Observation of Hydrofoil Cavitation", Proc. Spring Meeting Turbomachinery Society of Japan, pp27-32,in Japanese

(18) Goncalves E. et al.,2009," Numerical simulation of cavitating flows with homogeneous models", Computers & Fluids 38, pp1682–1696

(19) Frikha S. et al.,2008," Influence of the CavitationModel on the Simulation of Cloud Cavitation on 2D Foil Section", International Journal of Rotating Machinery, Volume 2008, Article ID 146234

(20) Kawamura T. et al.,2003,"Compariosn of Bubble and Sheet Cavitation Models for Simulation of Cavitating Flow over Hydrofoil",CAV2003 Osaka, Cav03-OS-1-008

(21) Masuda et al.,2007,"Multiscale Gas Liquid mixed phase flow analysis by a coupled interface capturing and Multi-fluid model",Proc. Mech. Eng. Congress JSME Vol.8,pp153-153,in Japanese

(22) Apte,S.V. et al.,"A Hybrid Lagrangian-Eulerian Approach for Simulation of Bubble Dynamics", CAV2009 Ann Arbor, Paper No.74

(23) Saito N. et al.,2000,"Direct numerical simulation of pool boiling",14th Symp. JSCFD,F08-1, in Japanese

(24) Reitz, R. D.,1987, "Modeling Atomization Process in High-Pressure Vaporizing Sprays", Atomization and Sprays Technology, Vol. 3, pp.309-337

(25) Takemura F et al.,(1992),"Effect if Internal Phenomena on Bubble Motion(2nd Report, Effects of transport Phenomena and Mist Formation Inside Bubble at the Expanding Phase)",Trans. JSME Series B,Vol.58,No.551,pp20-27,in Japanese